Cargo binding activates myosin VIIA motor function in cells

Tsuyoshi Sakai, Nobuhisa Umeki, Reiko Ikebe, and Mitsuo Ikebe[1]

Department of Microbiology and Physiological Systems, University of Massachusetts Medical School, Worcester, MA 01655

Edited* by James A. Spudich, Stanford University School of Medicine, Stanford, CA, and approved March 18, 2011 (received for review July 12, 2010)

Myosin VIIA, thought to be involved in human auditory function, is a gene responsible for human Usher syndrome type 1B, which causes hearing and visual loss. Recent studies have suggested that it can move processively if it forms a dimer. Nevertheless, it exists as a monomer in vitro, unlike the well-known two-headed processive myosin Va. Here we studied the molecular mechanism, which is currently unknown, of activating myosin VIIA as a cargo-transporting motor. Human myosin VIIA was present throughout cytosol, but it moved to the tip of filopodia upon the formation of dimer induced by dimer-inducing reagent. The forced dimer of myosin VIIA translocated its cargo molecule, MyRip, to the tip of filopodia, whereas myosin VIIA without the forced dimer-forming module does not translocate to the filopodial tips. These results suggest that dimer formation of myosin VIIA is important for its cargo-transporting activity. On the other hand, myosin VIIA without the forced dimerization module became translocated to the filopodial tips in the presence of cargo complex, i.e., MyRip/Rab27a, and transported its cargo complex to the tip. Coexpression of MyRip promoted the association of myosin VIIA to vesicles and the dimer formation. These results suggest that association of myosin VIIA monomers with membrane via the MyRip/Rab27a complex facilitates the cargo-transporting activity of myosin VIIA, which is achieved by cluster formation on the membrane, where it possibly forms a dimer. Present findings support that MyRip, a cargo molecule, functions as an activator of myosin VIIA transporter function.

ATPase | actomyosin | melanosome | regulation | retinal pigmented epithelium

Myosin VIIA is a member of the myosin superfamily. The mutant gene of myosin VIIA is responsible for human Usher syndrome type 1B (1) and two forms of nonsyndromic deafness, DFNB2 and DFNA11 (2–4). The heavy chain of this myosin has several structural characteristics. The N-terminal domain is a conserved motor domain followed by the neck domain containing five IQ motifs that binds light chains. The tail domain consists of a proximal segment of short predicted coiled-coil domain followed by a globular domain. Because of the presence of the coiled-coil domain, it was originally assumed that myosin VIIA exists as a dimer, i.e., a two-headed structure. However, recent biochemical and structural studies have revealed that myosin VIIA is a monomer (5, 6). The globular tail domain contains two large repeats, each incorporating a myosin tail homology 4 (MyTH4) domain and a band 4.1, ezrin, radixin, moesin (FERM) domain (7) (Fig. S1).

Myosin VIIA function is best studied in sensory organs. Myosin VIIA is found in two retinal cell types: the photoreceptor cells and the pigmented epithelial (RPE) cells (8, 9). Melanosomes in RPE cells undergo light cycle–dependent movement. After light onset, there was a significant increase in the number of melanosomes in the apical processes, and it is suggested that myosin VIIA is required for the proper movement of melanosome transportation (10).

A critical question is how the cargo-transporting activity can be regulated in cells. Because the tail domain is assumed to be the cargo-binding domain, we hypothesized that the myosin VIIA targeting molecules can serve as regulators of the myosin VIIA function. Among various myosin VIIA targeting molecules, the role of MyRip in melanosome transport has been best studied. In RPE cells, myosin VIIA, MyRip, and Rab27a are associated with melanosomes and motile small vesicles (11), suggesting that the ternary complex may function in melanosome motility.

In the present study, we observed the translocation of myosin VIIA and its cargos to the tip of filopodia and found that myosin VIIA is predominantly monomeric in cells, and it translocates to filopodial tips with its cargo molecule upon dimer formation. The cargo molecules, MyRip/Rab27a, induced the translocation of the wild-type myosin VIIA to the filopodial tips, suggesting that the cargo molecules play a critical role in activating myosin VIIA as a cargo transporter.

Results

Human Myosin VIIA Translocates to the Tip of Filopodia upon Dimer Formation. Recent studies have shown that *Drosophila* myosin VIIA is a monomeric (single-headed) myosin (5, 6). To examine whether human myosin VIIA in cells is predominantly monomer or dimer, we expressed the headless human myosin VIIA in cells from a spontaneously arising human RPE cell line, ARPE-19, and dimer formation was studied by using chemical cross-linking as a probe for dimer formation. As shown in Fig. 1*A*, M7SAHcoilTail, containing its endogenous short predicted coiled-coil region, could not be cross-linked. By contrast, dimer formation was efficiently demonstrated for M7SAHcoilTail with a leucine zipper motif (LZ-M7SAHcoilTail), forcing dimer production. We generated human myosin VIIA heavy meromyosin (M7HMM) constructs with a C-terminal FK506 binding protein (FKBP) that conditionally forms homodimers upon addition of the dimer-inducing drug AP20187 (12). This construct was efficiently cross-linked into the high-molecular-mass dimer only when the cells were incubated with AP20187 (Fig. 1*B*). As expected, dimers were similarly observed when the leucine zipper motif was added to the C-terminal end of M7HMM (M7HMM-LZ) (Fig. 1*B*). We also observed that endogenous myosin VIIA of ARPE-19 cells was not cross-linked, whereas myosin IIB in the cells was cross-linked to form a dimer (Fig. 1*C*). These results suggest that human myosin VIIA does not form a stable dimer in cells. It was reported previously that *Drosophila* myosin VIIA is a high duty ratio motor suitable for a processive movement (13), and the forced dimer of the tail-truncated *Drosophila* myosin VIIA can move processively in vitro (14). Therefore, we asked whether human myosin VIIA may move on actin filaments in vivo once it forms a dimer. As shown in Fig. 1*D*, we found that GFP-M7HMM-LZ, but not GFP-M7HMM without the leucine zipper, localized at the tip of filopodia. These results suggest that the GFP-M7HMM moves on actin-filament bundles within filopodia to the tip only when it forms a dimer.

To further address this notion, we used a drug-induced dimerization technique that we have described previously (12). The

Author contributions: T.S. and M.I. designed research; T.S. and N.U. performed research; T.S. and R.I. contributed new reagents/analytic tools; T.S. and M.I. analyzed data; and T.S. and M.I. wrote the paper.

The authors declare no conflict of interest.

*This Direct Submission article had a prearranged editor.

[1]To whom correspondence should be addressed. E-mail: mitsuo.ikebe@umassmed.edu.

This article contains supporting information online at www.pnas.org/lookup/suppl/doi:10.1073/pnas.1009188108/-/DCSupplemental.

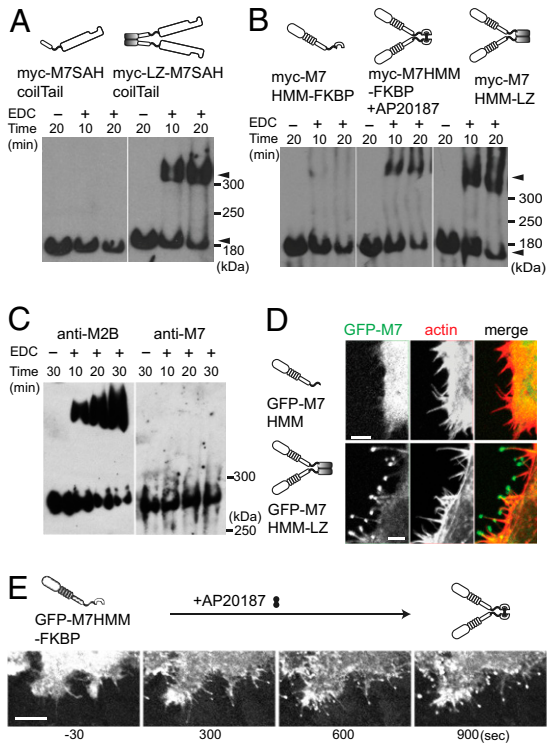

Fig. 1. Dimer formation induces the filopodial tip localization of human myosin VIIA in cells. (*A*) Cross-linking of myosin VII tail having the predicted coil domain. ARPE-19 cells were transfected either with myc-M7SAH/coil/Tail or myc-M7SAH/coil/Tail/LZ (three tandem copies of GCN4 sequence), and the cell extracts were subjected to cross-linking with 50 mM EDC [1-ethyl-3-(3-dimethylaminopropyl)carbodiimide hydrochloride] for 10 or 20 min, and the products were analyzed by Western blotting using anti-myc antibodies. Dimer and monomer of myc-M7SAH/coil/Tail are indicated by arrowheads. (*B*) Cross-linking of M7HMM constructs. ARPE-19 cells were transfected with either Myc-M7HMM-FKBP or myc-M7HMM-LZ. Cells were incubated with or without the dimer inducer, AP20187, and the cell extracts were subjected to cross-linking. Arrowheads indicate the dimer and monomer. (*C*) Cross-linking of endogenous myosin VIIA and myosin IIB in ARPE cells extracts. (*D*) M7HMM with, but not without, the leucine zipper motifs (three tandem copies of GCN4 sequence) localizes at the tip of filopodia. HeLa cells were transfected with GFP-M7HMM (*Upper*) or GFP-M7HMM-LZ (*Lower*). (*E*) Time-lapse images of dimerizer-induced translocation of GFP-M7HMM. The movement of GFP-M7HMM-FKBP in living HeLa cells was monitored under the confocal epifluorescence microscope after the addition of 100 nM AP20187 to the culture medium (Movie S1).

movement of GFP-M7HMM-FKBP in living HeLa cells was monitored under the confocal epifluorescence microscope. GFP-M7HMM-FKBP was distributed throughout the cell body before addition of the homodimerizer, AP20187 (Fig. 1*E Left*). However, after the addition of AP20187, GFP signals became progressively concentrated at the tip of filopodia over time (Fig. 1*E Right* and Movie S1). These results further support the notion that dimer formation is critical for the movement of myosin VIIA to the tip of filopodia. It should be noted that the overexpression of GFP-M7HMM-FKBP did not induce filopodia/microspike formation after the addition of AP20187 (Fig. S2), unlike myosin X (12, 15). In 3D images from confocal optical slices (Fig. S3), we found that GFP-M7HMM-FKBP also translocated toward the tip of apical filopodia. These results suggest that dimer formation is critical for the movement of myosin VIIA to filopodial tips of both substrate-attached and -nonattached apical filopodia.

Motor Activity and a Proper Neck Length Are Required for the Translocation of Myosin VIIA to the Tip of Filopodia. To see whether the translocation of GFP–myosin VIIA to the tip of filopodia is driven by the motor activity of myosin VIIA or by other mechanisms, we produced myosin VIIA constructs having an FKBP module, in which the residues critical for the motor activity are mutated (Fig. S4*A*). Three mutants were made: R212A, G440A, and G25R. The mutation of conserved R212 in Switch-1, which is critical for ATP binding, is expected to disrupt proper ATP-induced dissociation of myosin from actin upon ATP binding (16, 17). The conserved G440 is in the Switch-2 region, and the G440A mutation disrupts ATP hydrolysis but not the ATP binding–induced dissociation of myosin from actin (16, 18). On the other hand, the mutation of G25 (19), which is unique in myosin VII, inhibits the actin-activated ATPase activity of myosin VIIA (19). All three mutants failed to allow the translocation of GFP-M7HMM-FKBP to the tip of filopodia upon addition of AP20187. These results indicate that the translocation of GFP-M7HMM to the tips is driven by its own motor activity. Because dimer formation is critical for tip translocation, we suggest that the processive movement of myosin VIIA within filopodia is critical for tip translocation.

It has been thought that the neck length, or lever-arm length, may be important for the processive movement of myosin Va (20–25), myosin VI (26–28), and myosin X (12). Therefore, we examined whether the proximal tail domains, including the short coiled-coil and single α-helix (SAH) domains, are important for tip translocation of myosin VIIA. These domains may contribute to the lever-arm length. When we sequentially deleted two proximal tail domains, i.e., the coiled-coil and SAH domains, we found that, although the coiled-coil domain was dispensable for tip translocation, further truncation of the SAH domain abolished the translocation of GFP-M7HMM-FKBP (Fig. S4*B*). These results suggest that the SAH domain is important for the continuous movement of myosin VIIA within filopodia. Myosin VIIA has a long neck with five IQ motifs, similar to myosin Va with six IQ motifs, but our result suggests that the long IQ domain of myosin VIIA is not sufficient for processive movement.

Myosin VIIA Transports MyRip to the Tip of Filopodia upon Dimer Formation. To determine whether myosin VIIA can function as a cargo transporter, we cotransfected HeLa cells with GFP–myosin VIIA and mCherry-MyRip, a myosin VIIA binding protein (29, 30). GFP-M7HMMΔcoil-FKBP-tail, having the cargo-binding tail domain, showed diffuse localization before the addition of AP20187 (Fig. S5*A*), but it translocated to filopodial tips after the addition of the dimer inducer (Fig. S5*B*). On the other hand, mCherry-MyRip, showing diffuse localization before the addition of AP20187, translocated to filopodial tips after addition of AP20187 (Figs. S5*B* and S6). The transportation of MyRip required the tail domain of myosin VIIA because GFP-M7HMM-FKBP failed to transport mCherry-MyRip to the tip upon addition of AP20187, although it translocated to the tip upon the addition of AP20187 (Fig. S5*C*). However, in the absence of an FKBP or leucine zipper dimerization domain, GFP-M7Full was unable to cotransport mCherry-MyRip to the filopodial tips (Fig. S5*D*). These results suggest that a full-length myosin VIIA, once dimerized, can transport MyRip.

Myosin VIIA and MyRip Cotransported to the Filopodial Tips in ARPE-19 Cells. It has been suggested that myosin VIIA is present in RPE cells and may play an important role in transportation of melanosomes (10, 11, 16, 31). Using the RPE-derived cell line ARPE-19, we studied the translocation of myosin VIIA and its cargo molecule, MyRip. Expressed by itself, GFP-M7Full showed diffuse localization with no obvious tip localization (Fig. 2*A*). Quite interestingly, coexpression of mCherry-MyRip with GFP-M7Full induced the localization of both proteins to filopodial tips in cells (Fig. 2 *B* and *E*). Filopodial tip localization of GFP-M7Full was markedly increased from 4.3 ± 1.0% to 56 ± 5% by coexpression of mCherry-MyRip (Fig. 2*E*). As shown in Fig. S7, ARPE-19 cells

CELL BIOLOGY

express endogenous myosin VIIA. On the other hand, endogenous MyRip was not detected by Western blotting using anti-MyRip antibodies, which recognized GFP-MyRip expressed in transfected ARPE-19 cells. Therefore, we examined whether MyRip also induces the translocation of endogenous myosin VIIA. Expression of GFP-MyRip caused the filopodial tip localization of endogenous myosin VIIA along with GFP-MyRip (Fig. 2*C*), whereas filopodial tip localization of endogenous myosin VIIA was not observed in the absence of MyRip expression (Fig. 2*D*).

MyRip is known to associate with Rab27a, which binds to lipid vesicles with its geranyl-geranyl moiety (29, 30). We next asked whether Rab27a is also transported to filopodial tips along with MyRip. The cells were transfected with three constructs: GFP-M7Full, mCherry-MyRip, and myc-Rab27a. The triple transfection revealed that Rab27a was cotransported with myosin VIIA and MyRip to the tips of filopodia (Fig. 3*A*). Filopodial tip localization of GFP-M7Full was significantly increased from 5.5 ± 2.1% to 43.9 ± 5.7% by coexpression of mCherry-MyRip (Fig. 3*C*). The tip localization of myc-Rab27a required mCherry-MyRip (Fig. 3*B*), suggesting that MyRip bridges an association between myosin VIIA and Rab27a. The critical finding is that full-length myosin VIIA translocated to the tip of filopodia in the presence, but not in the absence, of MyRip. Because dimer formation is required for the filopodial tip localization of myosin VIIA, the results also suggest that the binding of MyRip may induce the dimer formation of myosin VIIA.

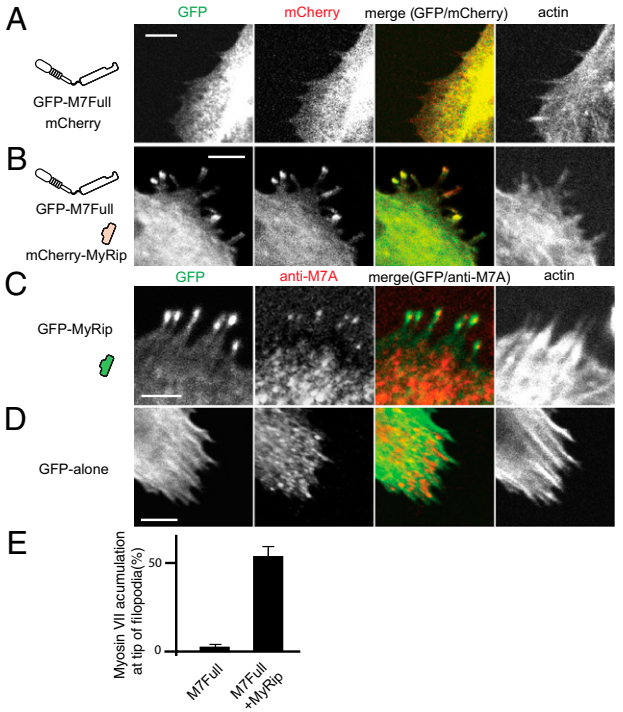

Fig. 2. MyRip induces the filopodia localization of full-length myosin VIIA in ARPE-19 cells. (*A*) GFP-M7Full alone without a forced dimerization motif did not localize at the tip of filopodia. GFP-M7Full was cotransfected with mCherry vector alone. Actin was stained with Alexa Fluor 568/phalloidin. (*B*) MyRip expression induces filopodial tip localization of GFP-M7Full. GFP-M7Full was cotransfected with mCherry-MyRip. (*C*) GFP-MyRip expression induces filopodial tip localization of endogenous myosin VIIA. (*D*) GFP alone expression did not induce filopodial tip localization of endogenous myosin VIIA. (*E*) Statistical analysis of the effect of MyRip on the filopodial tip accumulation of myosin VIIA. The numbers of filopodia with and without GFP–myosin VIIA at tips were counted. Values from three independent experiments are represented as mean ± SD (percentage of myosin VIIA at the tips): GFP–M7Full + mCherry vector alone, 4.0 ± 1.0%, *n* = 688; GFP–M7Full + mCherry-MyRip, 56.0 ± 4.9%, *n* = 973. (Bars = 10 μm.)

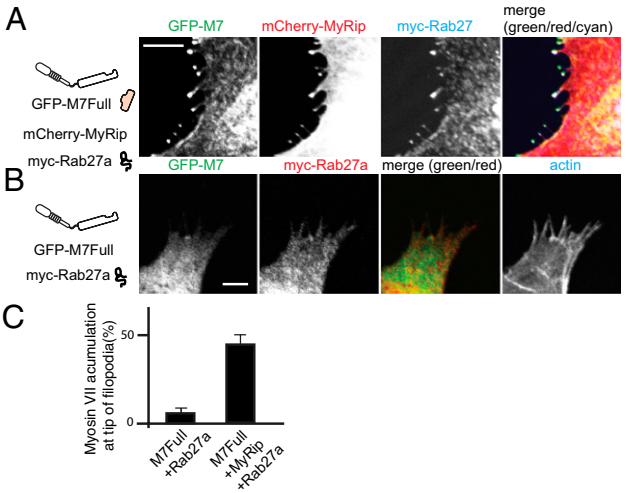

Fig. 3. Rab27a translocated with myosin VIIA and MyRip to the tip of filopodia. (*A*) Myosin VIIA transported MyRip together with Rab27a to the tip of filopodia. GFP-M7Full, mCherry-MyRip, and myc-Rab27a were coexpressed and stained with myc antibody followed by Alexa 647–labeled anti-mouse antibody. (*B*) Myc-Rab27a expression without mCherry-Rab27a did not induce the tip of filopodia localization of GFP-M7Full. (Bars = 10 μm.) (*C*) Statistical analysis of myosin VIIA accumulation at the filopodial tips. The numbers of filopodia with and without the tip localization of GFP–M7Full were counted. Right bar: GFP-M7Full + HA-MyRip + myc-Rab27; left bar: GFP-M7Full + myc-Rab27. Myc-Rab27 was stained with myc antibody followed by Alexa 568–labeled anti-mouse antibody. Actin was stained with Alexa Fluor 647. Values from three independent experiments are represented as mean ± SD. GFP-M7Full + HA-MyRip + myc-Rab27, 43.9 ± 5.7%, *n* = 342; GFP-M7Full + myc-Rab27, 5.5 ± 2.1%, *n* = 235.

MyRip Facilitates Association of Myosin VIIA to Vesicles and Promotes Dimer Formation. Because a myosin VIIA forced dimer, but not monomer, translocates to the filopodial tips, we hypothesized that the role of MyRip is to facilitate myosin VIIA association to membrane vesicles through Rab27a, which subsequently induces myosin VIIA dimer formation.

To evaluate this idea, we cotransfected MyRip and myosin VIIA tail in ARPE-19 cells. The cell lysates were subjected to cell fractionation. Separation of each fraction was confirmed by using the specific marker protein antibodies (Fig. 4*A*). The amount of myosin VIIA tail associated with membrane vesicle notably increased in the cells cotransfected mCherry-MyRip (Fig. 4*B*). The increase in the membrane-vesicle association in the presence of MyRip was calculated by considering the cotransfection efficiency (86 ± 3.5%, *n* = 4). We found that the membrane-vesicle association of myosin VIIA tail was significantly increased by 2.8 ± 0.6-fold in the presence of MyRip (*P* value of 0.0067 < 0.01 by paired *t* test) (Fig. 4*C*).

Next, we examined the effect of MyRip expression on myosin VIIA dimer formation by using a chemical cross-linking technique. As shown in Fig. 4*D*, the coexpression of MyRip produces cross-linked dimers of M7SAHcoilTail, in contrast to the expression of M7SAHcoilTail alone. The amount of the cross-linked dimer increased by 3.3 ± 0.4-fold in the presence of MyRip, considering the transfection efficiency (*P* value of 0.0065 < 0.01 by paired *t* test) (Fig. 4*E*). It should be noted that the amount of the cross-linked product of M7SAHcoilTail was much lower than that of LZ-M7SAHcoilTail, which contained the leucine zipper. We think that a significant fraction of M7SAHcoilTail in the cotransfected cells is monomeric even in the presence of GFP-MyRip, in part because only a part of M7SAHcoilTail associates

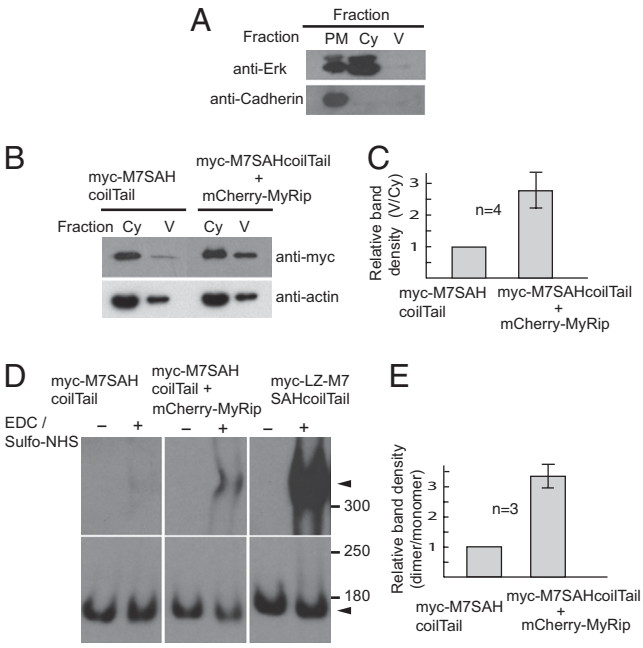

Fig. 4. MyRip promotes membrane recruitment and dimerization of myosin VIIA in ARPE-19 cells. ARPE-19 cells were either transfected with myc-M7SAHcoilTail or cotransfected with mCherry-MyRip and myc-M7SAHcoilTail. Plasma membrane–enriched fraction (PM), cytoplasmic soluble fraction (Cy), and small vesicle-containing fraction (V) were separated as described in *SI Materials and Methods*) Western blotting of each fraction using the antibodies against the marker proteins, Erk (extracellular signal-regulated kinase) (cytoplasmic marker), and *N*-cadherin (plasma membrane marker). (*B*) MyRip promotes the recruitment of myosin VIIA to membrane vesicles. The amount of myc-M7SAHcoilTail in cytoplasmic fraction (Cy) and small vesicle-containing fraction (V) were analyzed by Western blotting using anti-myc antibodies. Actin staining was done by using anti-actin antibodies as loading control. (*C*) The statistical representation of the effect of MyRip on membrane-vesicle recruitment of myc-M7SAHcoilTail. Band density of small vesicle-containing fraction (V) is denominated with the band density of cytoplasmic fraction (Cy). The band density was quantitated with ImageJ software. The value was normalized by using the transfection efficiency of myc-M7SAHcoilTail and mCherry-MyRip. The value of the cell extracts obtained from cells expressing myc-M7SAHcoilTail alone was taken to be 1. Error bars show ± SD from four independent experiments. (*D*) The effect of MyRip on myosin VIIA dimer formation revealed by chemical cross-linking. ARPE-19 cells were cotransfected with the indicated combinations of plasmids encoding myosin VIIA tail and MyRip. The cell extracts were subjected to cross-linking with 0 or 15 mM EDC/sulfo-NHS (*N*-hydroxysulfosuccinimide) (1:1) for 5 min. The products were analyzed by Western blotting using anti-myc antibodies. Dimer and monomer of myc-M7 tail constructs are indicated by arrowheads. The exposure time of monomer bands are shorter than dimer bands. (*E*) The statistical representation of the effect of MyRip on dimer formation. Band density of dimer was denominated with the band density of monomer. The value of the cell extracts obtained from myc-M7SAHcoilTail alone expressing cells was taken to be 1. Error bars show ± SD from three independent experiments. The mean values were normalized by using the cotransfection efficiency of myc-M7SAHcoilTail and mCherry-MyRip.

with MyRip/Rab27a complex. Supporting this view, we found that the amount of myosin VIIA tail in cytosol was much higher than that associated with vesicles, which represented myosin VIIA fraction associated with MyRip/Rab27a (Fig. 4*B*). The present results strongly suggest that the binding of MyRip to myosin VIIA induces the association of myosin VIIA to membrane vesicles and myosin VIIA dimer formation in ARPE-19 cells.

Elimination of Myosin VIIA/MyRip Interaction or MyRip/Rab27a Interaction Hampers Myosin VIIA Translocation to Filopodial Tips. The present results suggest that the formation of myosin VIIA/MyRip/Rab27a complex and its association with membrane vesicles is critical for myosin VIIA movement to the filopodial tips. To further evaluate this idea, we produced several deletion constructs of MyRip and Rab27a in which the domains critical to the attachment of myosin VIIA to membrane vesicles were eliminated. The effect of deletion on the translocation of myosin VIIA to the tip of filopodia was subsequently examined. The deletion of the C-terminal MyTH4 and FERM domain of myosin VIIA, the MyRip binding domain, diminished the translocation of myosin VIIA to the tip (Fig. 5 *A* and *D*). The deletion of the Fyve domain in MyRip, which serves as a Rab27a binding but not myosin VIIA binding site (29, 30), also hampered the tip localization of both myosin VIIA and MyRip (Fig. 5 *B* and *D*). These results further support the idea that the membrane targeting of myosin VIIA is critical for the movement of the myosin VIIA/cargo complex. On the other hand, the deletion of the short putative coiled-coil domain slightly decreased the tip localization of myosin VIIA (Fig. 5 *C* and *D*) (P value of $0.003 < 0.01$ by paired t test).

Discussion

Previous in vitro studies of *Drosophila* myosin VIIA have suggested that myosin VIIA can be a cargo-transporting motor because it is a high duty ratio motor (13) and the forced dimer construct of the tail-truncated *Drosophila* myosin VIIA moves processively in vitro (14). In the present study, we showed that human myosin VIIA can transport its cargo complex in ARPE-19 cells, thus functioning as a cargo transporter. Human myosin VIIA by itself showed diffuse localization, suggesting that myosin VIIA may not continuously move along actin structures toward the specific destination, such as filopodial tips, by itself in cells. The critical finding of the present study is that myosin VIIA moves cargoes to the tip of filopodia when it is forced to dimerize. The question is whether the wild-type full-length myosin VIIA, which is monomeric in vitro, can serve as a cargo transporter in cells. Although the wild-type full-length myosin VIIA did not localize at the filopodial tips, expression of MyRip in ARPE-19 cells induced the translocation of myosin VIIA along with MyRip (Fig. 2 *B* and *C*). Myosin VIIA, MyRip, and Rab27a are colocalized at the tip of filopodia (Fig. 3*A*), suggesting that myosin VIIA transports them after becoming activated by the binding to its cargo molecule complex.

Because Rab27a associates with membrane vesicles with its geranyl-geranyl moiety, it is thought that the MyRip/Rab27a complex links myosin VIIA to membrane vesicles, such as premature melanosomes, in ARPE-19 cells. It should be noted that, although ARPE-19 cells do not make mature melanosomes containing melanin (32), Rab27a is present at stages of melanosome maturation (33), which facilitates the translocation of myosin VIIA/cargo complex to the filopodial tips. Because a myosin VIIA forced dimer, but not monomer, can move toward filopodial tips, it is reasonable to assume that the production of myosin VIIA/MyRip/Rab27a ternary complex and its association with membrane vesicles induces dimer formation, thus activating the movement of myosin VIIA/cargo complex in cells. Supporting this view, we found that MyRip promotes membrane-vesicle association and dimer formation of myosin VIIA tail in ARPE-19 cells (Fig. 4). Because the production of a ternary complex is critical for myosin VIIA/cargo complex translocation, these results support the idea that the membrane targeting of myosin VIIA induces the cluster formation on the membrane, which facilitates possible dimer formation, which is critical for continuous movement of myosin VIIA and the activation of myosin VIIA as a cargo transporter to mediate trafficking of the melanosome/Rab27a/MyRip cargo complex.

Based on the present results, we propose the following model for the regulation of cargo transportation by myosin VIIA. Motor activity of myosin VIIA is inhibited before the binding of its cargo complex, and myosin VIIA binds to the adaptor molecules MyRip

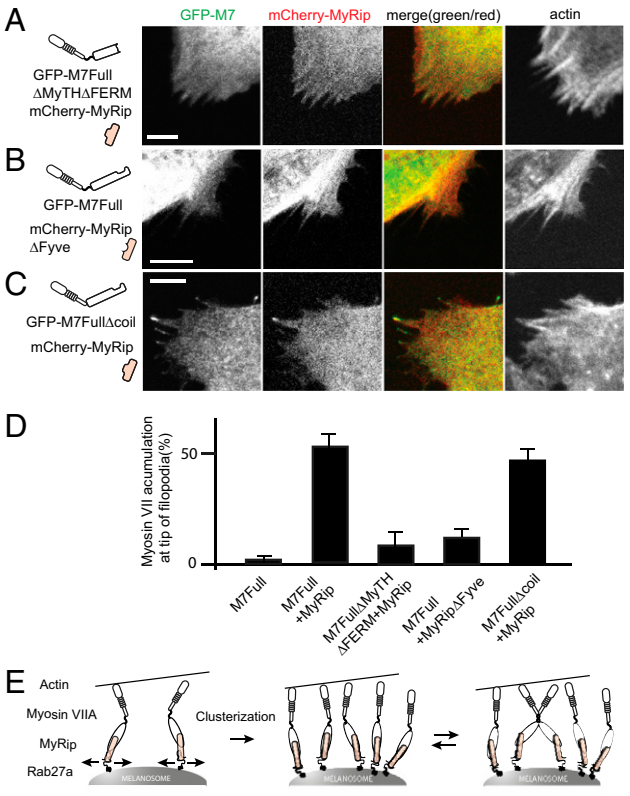

Fig. 5. Disruption of the formation of myosin VIIA/MyRip/Rab27a complex hampers translocation of myosin VIIA to filopodial tips. (*A*) Deletion of MyRip binding site (second MyTH-FERM domain) of myosin VIIA abolishes the translocation of myosin VIIA and MyRip to filopodial tips. (*B*) Deletion of the Rab27a binding site of MyRip (Fyve domain; 6–134 aa) hampers the translocation of myosin VIIA and MyRip to filopodial tips. (*C*) Effect of deletion of the predicted short coiled-coil domain of myosin VIIA on the translocation of myosin VIIA and MyRip to filopodial tips. Actin was stained with Alexa Fluor 647/phalloidin. (Bars = 10 μm.) (*D*) Statistical analysis of myosin VIIA accumulation at the filopodial tips. The numbers of filopodia with and without the tip localization of GFP–myosin VIIA were counted. First bar: GFP-M7Full + mCherry vector alone; second bar: GFP-M7Full + mCherry-MyRip; third bar: GFP-M7FullΔMyTHΔFERM + mCherry-MyRip; fourth bar: GFP-M7Full + mCherry-MyRipΔFyve; and fifth bar: GFP-M7FullΔcoil + mCherry-MyRip. Values from three independent experiments are represented as mean ± SD. GFP–M7Full + mCherry vector alone, 4.3 ± 1.0%, n = 688; GFP–M7Full + mCherry-MyRip, 56.0 ± 5.0%, n = 973; GFP–myosin VIIA ΔMyTHΔFERM + mCherry-MyRip, 11.9 ± 5.9%, n = 628; GFP–M7Full + mCherry-MyRipΔFyve, 15.9 ± 3.3%, n = 1,277; GFP–M7FullΔcoil + mCherry-MyRip, 49.0 ± 4.4%, n = 925. (*E*) Model that explains the cargo molecule–dependent regulation of myosin VIIA movement. Myosin VIIA bound to the adaptor molecules MyRip and Rab27a associates with membrane vesicles. On membrane vesicles, myosin VIIA monomers move laterally and encounter each other to form a cluster of molecules. When the molecules in the cluster come close enough to interact with each other, the two monomers form a dimer. Once myosin VIIA forms a cluster of molecules or a dimer, it carries the cargo to the filopodial tips.

and Rab27a. The binding to the adaptor molecules facilitates the association of myosin VIIA with membrane vesicles. Myosin VIIA monomers on membrane vesicles move laterally on the membrane and encounter each other to form a cluster of molecules, which may induce dimer formation, and the movement is activated. Alternatively, formation of a cluster of molecules may be sufficient to support continuous movement of the vesicles. Recently, it was reported that a cluster of four myosin VI molecules on a nanosphere can move the nanosphere processively on actin structure of the permeabilized cells (34). On the other hand, it has been thought that the motility of the KIF1/Unc-104 class of kinesin may be regulated by reversible monomer–dimer transition (35). Although Unc-104 in solution is monomeric, it has been suggested that the neck-linker undocking or saturation of microtubules with Unc-104 induces dimer formation (36, 37). Tomishige et al. showed that rapid processive motility of Unc-104 is observed only when the motor is artificially dimerized (38). In the case of Unc-104, the processive movement of a dimer cannot be substituted by a clustering of monomers. Further studies are required whether the dimer formation is absolutely necessary for cargo transportation by myosin VIIA.

For myosin VI, cargo proteins, such as Dab2 and optineurin, directly induced myosin VI dimer (39). The tail domain of myosin VI binds to the 39-residue fragment of the vesicle adaptor Dab2, which induces dimerization of the tail/Dab2 peptide complex (40). In the present study, it is suggested that, unlike myosin VI/Dab2 binding, the binding of the targeting molecule, MyRip, does not directly promote dimer formation. These results suggest that, although dimer formation is important for the cargo-transporting function of motor proteins, the regulatory mechanisms of dimer formation and, more importantly, the cargo-transporting function of motor proteins is different from each other.

The function of the predicted short coiled-coil domain is obscure. The deletion of this domain did not largely diminish the tip localization of myosin VIIA when MyRip was coexpressed in ARPE-19 cells (Fig. 5 *C* and *D*), and this region may not contribute to the dimer formation. This region also is not required for the motility activity of myosin VIIA itself because the deletion of this region does not hamper the movement of myosin VIIA forced dimer to the tip of filopodia (Fig. S4*B*). In contrast, the SAH domain is important to achieve the movement of myosin VIIA to the filopodial tips (Fig. S4*B*). It was shown for myosin Va that the shortening of the IQ domain diminishes the run length of myosin Va, suggesting that the length of IQ domain is important for processive movement of myosin Va (20, 22). Previously, we found that the deletion of the SAH region hampered the continuous movement of dimerized myosin X (12). Therefore, it is thought that the SAH region provides the sufficient length/flexibility of the neck to achieve continuous movement of dimerized myosin.

It was shown previously with melanophilin-depleted skin melanocytes that myosin VIIA overexpression alone failed to rescue the melanosome clustering phenotype, whereas coexpression of MyRip and myosin VIIA restored normal peripheral melanosome distribution (41). The present results are consistent with this earlier report. The presence of both myosin VIIA and MyRip are critical to showing the myosin VIIA–dependent phenotype, further suggesting that MyRip not only is a cargo but also plays a role in the activation of myosin VIIA as a cargo-transporting motor. In RPE cells in retina, it was reported that myosin VIIA and melanosomes are not highly localized at the tip of apical process (10, 42). The diameter of apical process is small compared with the elongated melanosomes in mature RPE cells (10). It is known that the majority of melanosomes were located below the apical region of the RPE (43), and it is thought that melanosomes below the apical process can absorb light effectively and completely, blocking the light coming from all directions. The distribution of melanosomes of the RPE at this location is very important to proper optical function. The present finding is consistent with the idea that myosin VIIA transports melanosomes to the base of apical process and localizes them to absorb light, which is critical for normal optical function.

Materials and Methods

Plasmid Construction. Myosin VIIA, MyRip, and Rab27a cDNAs were obtained from a human cDNA library, and the amino acid sequences were identical with the submitted sequences (GenBank accession nos. NM000260, NM015460, and BC136423). The FKBP-encoding fragment was PCR-amplified from pC4-Fv1E (ARIAD Pharmaceuticals) and subcloned into pEGFP-M7HMM to create pEGFP-M7HMM-FKBP. GFP-M7FullΔcoil-FKBP-tail was created by

swapping the FKBP fragment for the myosin VIIA coiled-coil domain (901–929 aa). pEGFP-M7FullΔcoil was generated by the PCR-mediated plasmid DNA deletion method. Myosin VIIA motor dead mutants (R212A and G457A) and Usher syndrome type 1B mutants (G25R) were created by site-directed mutagenesis (44). The other deleted myosin VIIA constructs and MyRipΔFyve were generated by PCR methods using appropriate sets of primers with restriction enzyme site. All expression plasmids were verified by DNA sequencing.

Chemical Cross-Linking of Cellular Extracts. ARPE-19 cells were transfected with the indicated constructs on 10-cm dishes. At 24 h after the transfection, the cells were washed with PBS and collected in a 1.5-mL tube. The cell pellets were snap-frozen with liquid nitrogen and stored at −80 °C. The cells were resuspended in 60 μL of Solution A [150 mM NaCl, 25 mM Hepes/NaOH (pH 7.4), 1 mM PMSF, 10 μg/mL leupeptin, 2 μg/mL pepstatin A, and 1 μg/mL trypsin inhibitor] and homogenized in a 1.5-mL tube with a pellet pestle (Kimble-Kontes) on ice. The samples were centrifuged at 22,000 × *g* for 5 min at 4 °C, and the supernatants were mixed with an equal volume of Solution B [1050 mM NaCl, 25 mM Hepes/NaOH (pH 7.4), 1 mM PMSF, 10 μg/mL leupeptin, 2 μg/mL pepstatin A, and 1 μg/mL trypsin inhibitor]. For the cross-linking of full-length myosin VIIA in ARPE-19 cells, 5 mM ATP and 0.5% Nonidet P-40 were added to Solutions A and B. After 1 min, the samples were incubated with 50 mM 1-ethyl-3-(3-dimethylaminopropyl)carbodiimide (EDC; Invitrogen) (Fig. 1 *A*–*C*) or with 15 mM EDC and 15 mM sulfo-NHS (Invitrogen) (Fig. 4*D*) at 25 °C. At the indicated time, the aliquots were immediately mixed with 1/2 vol of 0.1 M Tris containing SDS sample buffer [0.1 M Tris·HCl (pH 6.8), 4% SDS, 60% glycerol, 0.04% bromophenol blue, and 100 mM DTT] to stop the reaction. Proteins were separated on a 3.75% Weber–Osborn SDS/phosphate gels.

Further details on antibodies, Western blot analysis, cell culture and transfection, confocal microscopy, immunofluorescence staining, and subcellular fractionation are available in *SI Materials and Methods*.

ACKNOWLEDGMENTS. We thank Dr. E. Luna and Dr. R. Fenton for suggestions on the manuscript. This work is supported by National Institutes of Health Grants DC006103, HL073050, AR048526, and AR048898.

1. Weil D, et al. (1995) Defective myosin VIIA gene responsible for Usher syndrome type 1B. *Nature* 374:60–61.
2. Weil D, et al. (1997) The autosomal recessive isolated deafness, DFNB2, and the Usher 1B syndrome are allelic defects of the myosin-VIIA gene. *Nat Genet* 16:191–193.
3. Liu XZ, Newton VE, Steel KP, Brown SD (1997) Identification of a new mutation of the myosin VII head region in Usher syndrome type 1. *Hum Mutat* 10:168–170.
4. Liu XZ, et al. (1997) Mutations in the myosin VIIA gene cause non-syndromic recessive deafness. *Nat Genet* 16:188–190.
5. Umeki N, et al. (2009) The tail binds to the head-neck domain, inhibiting ATPase activity of myosin VIIA. *Proc Natl Acad Sci USA* 106:8483–8488.
6. Yang Y, et al. (2009) A FERM domain autoregulates *Drosophila* myosin 7a activity. *Proc Natl Acad Sci USA* 106:4189–4194.
7. Chen ZY, et al. (1996) Molecular cloning and domain structure of human myosin-VIIa, the gene product defective in Usher syndrome 1B. *Genomics* 36:440–448.
8. Hasson T, Heintzelman MB, Santos-Sacchi J, Corey DP, Mooseker MS (1995) Expression in cochlea and retina of myosin VIIa, the gene product defective in Usher syndrome type 1B. *Proc Natl Acad Sci USA* 92:9815–9819.
9. Liu X, Vansant G, Udovichenko IP, Wolfrum U, Williams DS (1997) Myosin VIIa, the product of the Usher 1B syndrome gene, is concentrated in the connecting cilia of photoreceptor cells. *Cell Motil Cytoskeleton* 37:240–252.
10. Futter CE, Ramalho JS, Jaissle GB, Seeliger MW, Seabra MC (2004) The role of Rab27a in the regulation of melanosome distribution within retinal pigment epithelial cells. *Mol Biol Cell* 15:2264–2275.
11. Klomp AE, Teofilo K, Legacki E, Williams DS (2007) Analysis of the linkage of MYRIP and MYO7A to melanosomes by RAB27A in retinal pigment epithelial cells. *Cell Motil Cytoskeleton* 64:474–487.
12. Tokuo H, Mabuchi K, Ikebe M (2007) The motor activity of myosin-X promotes actin fiber convergence at the cell periphery to initiate filopodia formation. *J Cell Biol* 179: 229–238.
13. Watanabe S, Ikebe R, Ikebe M (2006) *Drosophila* myosin VIIA is a high duty ratio motor with a unique kinetic mechanism. *J Biol Chem* 281:7151–7160.
14. Yang Y, et al. (2006) Dimerized *Drosophila* myosin VIIa: A processive motor. *Proc Natl Acad Sci USA* 103:5746–5751.
15. Berg JS, Cheney RE (2002) Myosin-X is an unconventional myosin that undergoes intrafilopodial motility. *Nat Cell Biol* 4:246–250.
16. Li XD, et al. (1998) Effects of mutations in the γ-phosphate binding site of myosin on its motor function. *J Biol Chem* 273:27404–27411.
17. Shimada T, Sasaki N, Ohkura R, Sutoh K (1997) Alanine scanning mutagenesis of the switch I region in the ATPase site of *Dictyostelium discoideum* myosin II. *Biochemistry* 36:14037–14043.
18. Kambara T, et al. (1999) Functional significance of the conserved residues in the flexible hinge region of the myosin motor domain. *J Biol Chem* 274:16400–16406.
19. Watanabe S, Umeki N, Ikebe R, Ikebe M (2008) Impacts of Usher syndrome type IB mutations on human myosin VIIa motor function. *Biochemistry* 47:9505–9513.
20. Sakamoto T, et al. (2003) Neck length and processivity of myosin V. *J Biol Chem* 278: 29201–29207.
21. Rief M, et al. (2000) Myosin-V stepping kinetics: A molecular model for processivity. *Proc Natl Acad Sci USA* 97:9482–9486.
22. Purcell TJ, Morris C, Spudich JA, Sweeney HL (2002) Role of the lever arm in the processive stepping of myosin V. *Proc Natl Acad Sci USA* 99:14159–14164.
23. Volkmann N, et al. (2005) The structural basis of myosin V processive movement as revealed by electron cryomicroscopy. *Mol Cell* 19:595–605.
24. Baboolal TG, et al. (2009) The SAH domain extends the functional length of the myosin lever. *Proc Natl Acad Sci USA* 106:22193–22198.
25. Kodera N, Yamamoto D, Ishikawa R, Ando T (2010) Video imaging of walking myosin V by high-speed atomic force microscopy. *Nature* 468:72–76.
26. Sun Y, et al. (2007) Myosin VI walks "wiggly" on actin with large and variable tilting. *Mol Cell* 28:954–964.
27. Reifenberger JG, et al. (2009) Myosin VI undergoes a 180° power stroke implying an uncoupling of the front lever arm. *Proc Natl Acad Sci USA* 106:18255–18260.
28. Dunn AR, Chuan P, Bryant Z, Spudich JA (2010) Contribution of the myosin VI tail domain to processive stepping and intramolecular tension sensing. *Proc Natl Acad Sci USA* 107:7746–7750.
29. El-Amraoui A, et al. (2002) MyRIP, a novel Rab effector, enables myosin VIIa recruitment to retinal melanosomes. *EMBO Rep* 3:463–470.
30. Fukuda M, Kuroda TS (2002) Slac2-c (synaptotagmin-like protein homologue lacking C2 domains-c), a novel linker protein that interacts with Rab27, myosin Va/VIIa, and actin. *J Biol Chem* 277:43096–43103.
31. Lopes VS, et al. (2007) The ternary Rab27a-Myrip-Myosin VIIa complex regulates melanosome motility in the retinal pigment epithelium. *Traffic* 8:486–499.
32. Dunn KC, Aotaki-Keen AE, Putkey FR, Hjelmeland LM (1996) ARPE-19, a human retinal pigment epithelial cell line with differentiated properties. *Exp Eye Res* 62: 155–169.
33. Jordens I, et al. (2006) Rab7 and Rab27a control two motor protein activities involved in melanosomal transport. *Pigment Cell Res* 19:412–423.
34. Sivaramakrishnan S, Spudich JA (2009) Coupled myosin VI motors facilitate unidirectional movement on an F-actin network. *J Cell Biol* 187:53–60.
35. Al-Bassam J, et al. (2003) Distinct conformations of the kinesin Unc104 neck regulate a monomer to dimer motor transition. *J Cell Biol* 163:743–753.
36. Rice S, et al. (1999) A structural change in the kinesin motor protein that drives motility. *Nature* 402:778–784.
37. Hoenger A, et al. (2000) A new look at the microtubule binding patterns of dimeric kinesins. *J Mol Biol* 297:1087–1103.
38. Tomishige M, Klopfenstein DR, Vale RD (2002) Conversion of Unc104/KIF1A kinesin into a processive motor after dimerization. *Science* 297:2263–2267.
39. Phichith D, et al. (2009) Cargo binding induces dimerization of myosin VI. *Proc Natl Acad Sci USA* 106:17320–17324.
40. Yu C, et al. (2009) Myosin VI undergoes cargo-mediated dimerization. *Cell* 138: 537–548.
41. Kuroda TS, Fukuda M (2005) Functional analysis of Slac2-c/MyRIP as a linker protein between melanosomes and myosin VIIa. *J Biol Chem* 280:28015–28022.
42. Futter CE (2006) The molecular regulation of organelle transport in mammalian retinal pigment epithelial cells. *Pigment Cell Res* 19:104–111.
43. Kim IT, Choi JB (1998) Melanosomes of retinal pigment epithelium—Distribution, shape, and acid phosphatase activity. *Korean J Ophthalmol* 12:85–91.
44. Weiner MP, et al. (1994) Site-directed mutagenesis of double-stranded DNA by the polymerase chain reaction. *Gene* 151:119–123.